Nozzle Design for Combined Use of MQL and Cryogenic Gas in Machining

Octavio Pereira[1,2,#], **Adrián Rodríguez**[1], **Joaquín Barreiro**[2], **Ana Isabel Fernández-Abia**[2], and **Luis Norberto López de Lacalle**[1]

1 University of the Basque Country (UPV/EHU), Department of Mechanical Engineering, C/Alameda de Urquijo s/n, Bilbao 48013, Spain
2 University of Leon (ULE), Department of Mechanical, Computing and Aerospace Engineering, Campus de Vegazana s/n, Leon 24071, Spain
Corresponding Author | Email: octaviomanuel.pereira@ehu.eus, TEL: +34-94-601-3932, FAX: +34-94-601-4215

Nowadays, the need for not only technically but also environmentally efficient machining processes is increasing. In this context, the reduction of oil emulsion type coolants used during machining of aeronautical engine components supposes a great challenge. In this paper, a novel approach based on the design, optimization and validation of a nozzle adaptor combining cryogenic technology and minimum quantity lubrication systems is proposed. The proposed work also deals with the aim of obtaining a cost-effective process. Thus, CO_2 flow and velocity was optimized in this line. Theoretically-based analysis were performed and compared with computational fluid dynamics (CFD) simulations and with real experimental tests as well. Once optimizing these key factors, two nozzle adaptors were designed and simulated by CFD. Different geometries were tested looking for the most efficient design. Finally, to obtain a feasible industrial product, the developed nozzle was tested as a CryoMQL demonstrator comparing with other lubri-coolant techniques during milling Inconel 718. Results show a successful balance between technical and environmental issues using this technology when milling aeronautical alloys.

1. Introduction

The use of heat-resistant alloys in aeronautical turbomachinery industry is growing worldwide. These alloys apart of working with high temperatures, they have to support extreme mechanical conditions. In particular, these alloys are characterized by properties such as: high strength in comparison with its weight; high elastic limit; high corrosion and erosion resistance; high hot strength and hardness and low conductivity. On the other hand, in machining processes, these advantages become in low material removal rates, high cutting forces, adhesion, welding and other problems on the cutting tool, and consequently premature tool wear.[1-5] Furthermore, surface integrity often is damaged by both thermal and mechanical effects.[6]

In order to avoid these problems, it is common to inject cutting fluids in the cutting zone. Generally, cutting fluids are composed by mineral/synthetic oil emulsions. They suppose over 17% of the total manufacturing costs.[7] Moreover, the amount consumed in the European Union is around 320.000 Tm/year. 30% of these cutting fluids are lost through leaks in circuits and/or in pieces cleaning processes. Thus, the treatment process when its useful life is finished results inefficient and

finally, this contamination ends up in rivers, natural springs and finally inside the alimentary chain.[8,9] Besides, the use of these cutting fluids implies problems in workers' health such as asthma or acne, pneumonia, and even skin or lung cancer.[10,11] In addition, this treatment process supposes between 2 and 4 times its purchase price,[12] what it is unacceptable due to the high industrial competitiveness. Thus, due to growing environmental consciousness and competitiveness as well as recent regulations,[13,14] it is being necessary to consider new alternative cooling-lubrication systems more efficient, cheap, reliable and environmentally sustainable.

An alternative to mineral/synthetic cutting fluids studied for last 15 years is minimum quantity lubrication technology (MQL). With this one, instead of using oil emulsions to inject in the cutting zone, biodegradable oil microparticles are sprayed. With this technique, oil flow rate is reduced until values between 10 mL/h and 100 mL/h. At the same time, oil penetration capacity in the cutting zone is enhanced and workers' health matters are solved.[15,16] However, despite MQL has good lubrication properties, cooling and evacuation chip capacities are lost, what makes technology insufficient to be applied on turbomachinery materials.
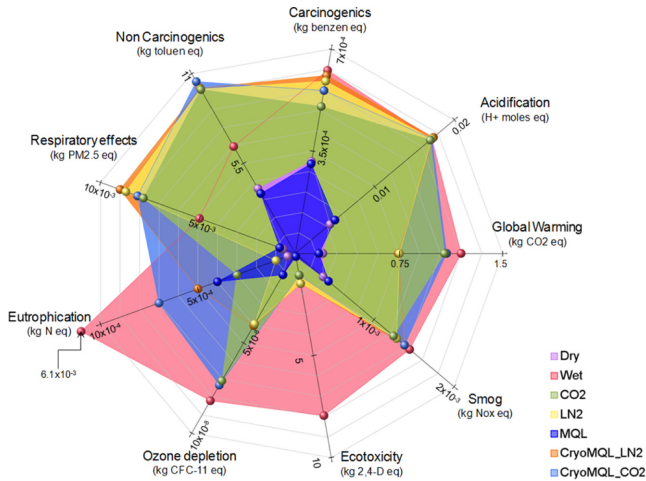
Springer

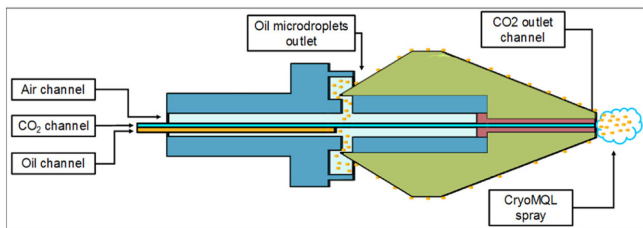Fig. 1 Cutting fluids environmental impact[17]

Fig. 2 Coanda effect nozzle[23]

At this point is where cryogenic technology was begun to investigate in machining operations. Cryogenic machining consists on injecting a liquefied gas in the cutting zone. Normally, the liquefied gases used are liquid nitrogen (LN_2) or liquid carbon dioxide (CO_2). It should be noted that CO_2 is obtained from a primary process, that is, CO_2 generated as waste in other process is used instead of exhausted directly to the atmosphere. In Fig. 1 is shown a complete life cycle assessment (LCA) in which is providing a comparison between different lubricooling technologies.[17] In this research, similar environmental impact was obtained for the two cryogenic gases. In fact, although CO_2 presents higher ozone depletion and global warming values, LN_2 presents higher carcinogenics and respiratory ones. Thus, environmental innocuousness associated to LN_2 cryogenic machining is maintained. On the other hand, cryogenic technology presents other advantages as: the gases purchase price is relatively cheap; cutting temperature is reduced; inert gases are used; it does not create waste; and it is completely harmless to workers' health. However, despite cryogenic technology is a good cooler, it does not provide enough lubrication, what it is important for being applied in most part of turbomachinery component alloys.

Thereby, the combination of both environmental friendly technologies seems to be the key. This technology, known as CryoMQL, joins both MQL and cryogenic advantages, that is, at the same time it lubricates and cools the cutting zone. Several investigations were carried out in this way, obtaining successful results on turbomachinery component alloys such as titanium or nickel alloys.[18-21] CryoMQL consists on mixing MQL oil microdroplets with CO_2 liquefied gas. In this line, there is two ways to obtain a cryogenic

spray. The first one is through dissolving oil in supercritical CO_2.[20-22] This process consists on heating CO_2 over its critical point in a pressured tank with oil. Then, the mixture is injected by a simple nozzle in the cutting zone. The other one is by a coanda effect nozzle.[23]

This nozzle is made up with three inlets and two outlets, as it is shown in Fig. 2. First outlet is in the middle of the nozzle body and the other is in the nozzle tip. Centre inlets carry CO_2, air and oil, respectively. CO_2 inlet carries it from the injection system to the nozzle tip.

Nevertheless, air and oil inlets discharge into an internal mix chamber where oil microparticles are generated by Venturi's effect. These microparticles reach the nozzle tip going across the outer nozzle wall by coanda effect. Once reached the nozzle tip, microparticles are dragged by the CO_2 jet. This nozzle is provided by "electrospraying" technology to ensure a better pulverization.

Although this combination is the most effective alternative to avoid the use of mineral/synthetic oil emulsions, it implies a considerable initial investment in CryoMQL regulation and injection systems. Therefore, a new nozzle adaptor is proposed to avoid these considerable initial expenses; maintain spray low temperatures and environmental harmlessness; and achieve a CryoMQL technology combining existing MQL systems with cryogenic ones.

For this purpose, several CO_2 outlet diameters were analyzed by computer fluid dynamics (CFD). Afterwards, these results were compared with empirical results obtained in a test bench to validate the mathematical basis used during CFD simulations. Besides, the minimum useful CO_2 velocity to be used during machining operations was obtained with this comparison. Then, basing on these previous tests, two nozzle adaptors were developed and analyzed by computer fluid dynamics (CFD). Finally with the adequate nozzle adaptor, CryoMQL technology was tested in comparison with other lubri-cooling technologies to be applied in turbomachinery alloys. In this line, Inconel 718 -a representative difficult to cut turbomachinery alloy- was milled. The results show that it is feasible to apply CryoMQL technology with the nozzle adaptor proposed during milling operations.

2. Mathematical Basis of the Simulations

The simulations were carried out through Fluent software. The CFD mathematical basis takes relevance for getting rapid convergences and realistic solutions. A bad combination between the method, the turbulence model and the iteration algorithm becomes in long simulations without solution convergence. Thus, a robust combination has to be chosen in order to achieve suitable simulations.

In this case, the Volume of Fluid model (VOF) was used to calculate the spray velocity and its concentration in the cutting zone. This model is characterized by offering the possibility of modelling two or more immiscible fluids with different fluid velocities. In this model, the control volumes must be defined by a simple phase fluid or their combinations, that is, there cannot be nodes without mass.

In contrast to other CFD models in which the mass, momentum and energy conservation equations are solved, in VOF model conservation mass equation is replaced by volume fraction equation in each node modelled. Therefore for a phase q, if its volume fraction in the cell is α_q, three situations are possible:

· $\alpha_q = 0$, the cell is empty of this fluid.

· $\alpha_q = 1$, the cell is full with the fluid q.

· $0 < \alpha_q < 1$, the cell contains the fluid q and one or more fluids until the sum of each volume fraction to be the unity.

Based on the local value α_q, properties and variables are assigned to each control volume within the domain. Volume fraction equation is represented in Eq. (1). In the right side, m_{qp} and m_{pq} are the mass transfer from "q" phase to "p" phase and vice versa, and $S_{\alpha q}$ is the mass source term for phase q. In the left side, ρ_q and v_q are the density and velocity of the phase q.

$$\frac{1}{\rho_q}\left[\frac{\partial}{\partial t}(\alpha_q \rho_q) + \nabla \cdot (\alpha_q \rho_q \vec{v_q}) = S_{\alpha q} + \sum_{p=1}^{n}(\dot{m}_{pq} - \dot{m}_{qp})\right] \qquad (1)$$

Regarding momentum equation, only it is solved throughout the domain, and resulting velocity field is shared among the phases, as it is shown in Eq. (2). As it can be seen, the momentum equation is dependent on the volume fractions of all phases through density (ρ) and viscosity (μ). In this case, g is the gravitational acceleration and F is a source term which accounts for surface tension effects.

$$\frac{\partial}{\partial t}(\rho\vec{v}) + \nabla \cdot (\rho\vec{v}\vec{v}) = -\nabla p + \nabla \cdot [\mu(\nabla\vec{v} + \nabla\vec{v}^T)] + \rho\vec{g} + \vec{F} \qquad (2)$$

Energy equation, also shared among the phases, is shown in Eq. (3). In this case, energy (E) and temperature (T) are considered as mass-average variables in each node. This average is represented in Eq. (4) for the energy variable, where E_q for each phase is based on the specific heat of that phase and the shared temperature; K_{eff} is the effective thermal conductivity; and S_h is a variable to have into account the radiations, as well as any other volumetric heat sources.

$$\frac{\partial}{\partial t}(\rho E) + \nabla \cdot (\vec{v}(\rho E + p)) = \nabla \cdot (k_{eff}\nabla T) + S_h \qquad (3)$$

$$E = \frac{\sum_{q=1}^{n} \alpha_q \rho_q E_q}{\sum_{q=1}^{n} \alpha_q \rho_q} \qquad (4)$$

Other physical properties, such as density and viscosity, are calculated by the presence of each phase in each node. For example, in Eq. (5) is shown the volume-fraction-average density.

$$\rho = \sum \alpha_q \rho_q \qquad (5)$$

Regarding different turbulence models, turbulence "K-ε Realizable" model proposed by Shih et al.[24] was chosen. This turbulence model is a RANS model (Navier-Stokes) based in two-equation viscous vorticity models. Initial and/or boundary conditions are needed as input parameters. This selected model was established and fully validated in numerous and well-known scientific papers.[25-27] However, in comparison with other "K-ε" models, this model presents substantial improvements in flow characteristics -including a strong aerodynamic curvature- and avoids production of negative energy components. Its transport turbulence kinetic energy is shown in Eq. (6), where $\frac{\partial}{\partial t}(\rho k)$ is

the rate of change of mean kinetic energy (K); $\frac{\partial}{\partial x_j}(\rho k u_j)$ is the transport of K by convection; $\frac{\partial}{\partial x_j}\left[\left(\mu + \frac{\mu_t}{\sigma_k}\right)\frac{\partial k}{\partial x_j}\right]$ is the transport of K by diffusion, where σ_k is 1.0; P_k is the K generation due to main velocity gradient; P_b is the K generation due to floatability; $\rho\varepsilon$ is ε dissipation rate; Y_M represents the contribution of the fluctuating dilation in compressible turbulence to the overall dissipation rate.

$$\frac{\partial}{\partial t}(\rho k) + \frac{\partial}{\partial x_j}(\rho k u_j) = \frac{\partial}{\partial x_j}\left[\left(\mu + \frac{\mu_t}{\sigma_k}\right)\frac{\partial k}{x_j}\right] + P_k + P_b - \rho\varepsilon - Y_M \qquad (6)$$

This model is characterized by a modified transport equation for kinetic energy dissipation rate (ε) which is based on an exact equation for the transport of mean-square vorticity fluctuation. The new transport equation for ε is shown in Eq. (7), where $\frac{\partial}{\partial t}(\rho\varepsilon)$ is the rate of change of ε; $\frac{\partial}{\partial x_j}(\rho\varepsilon u_j)$ is the transport of ε by convection; $\frac{\partial}{\partial x_j}\left[\left(\mu + \frac{\mu_t}{\sigma_\varepsilon}\right)\frac{\partial \varepsilon}{\partial x_j}\right]$ is the transport of ε by diffusion, where σ_ε is 1.2; $\rho C_1 S\varepsilon - \rho C_2 \frac{\varepsilon^2}{k + \sqrt{v\varepsilon}}$ is the dissipation rate equation of ε, where C_1 is governed by Eq. (8) and C_2 is Eqs. (1) and (9); and is the generation rate equation of ε, where $C_{1\varepsilon}$ is 1.44.

$$\frac{\partial}{\partial t}(\rho\varepsilon) + \frac{\partial}{\partial x_j}(\rho\varepsilon u_j)$$
$$= \frac{\partial}{\partial x_j}\left[\left(\mu + \frac{\mu_t}{\sigma_\varepsilon}\right)\frac{\partial \varepsilon}{\partial x_j}\right] + \rho C_1 S\varepsilon - \rho C_2 \frac{\varepsilon^2}{k + \sqrt{v\varepsilon}} + C_{1\varepsilon}\frac{\varepsilon}{k}C_{3\varepsilon}P_b \qquad (7)$$

$$C_1 = \max\left[0.43, \frac{\eta}{\eta + 5}\right] \qquad (8)$$

where:

$$\eta = S\frac{k}{\varepsilon}; \quad S = \sqrt{2S_{ij}S_{ij}}; \quad S_{ij} = \frac{1}{2}\left(\frac{\partial u_j}{\partial x_i} + \frac{\partial u_i}{\partial x_j}\right)$$

Furthermore, instead of using a constant turbulent viscosity, it is governed by Eq. (9). This equation introduces the variable proposed originally by Reynolds[25] and after developed by Shih and Zhu[29], C_μ, which is shown in Eq. (10). In this equation, main flow (U*) is defined by Eq. (11) which takes into account the anisotropic strain rate (S_{ij}) and the mean rotation rate viewed in the rotating reference fame ($\tilde{\Omega}_{ij}$); A_s coefficient, which depends on the strain type, is defined by Eq. (12); and A_0 value is 4.04 in order to produce the proper level of shear stress in shear flow.

$$\mu_t = \rho C_\mu \frac{k^2}{\varepsilon} \qquad (9)$$

$$C_\mu = \frac{1}{A + A_S U^* \frac{k}{\varepsilon}} \qquad (10)$$

$$U^* \equiv \sqrt{S_{ij}S_{ij} + \tilde{\Omega}_{ij}\tilde{\Omega}_{ij}} \qquad (11)$$

where:

$$\tilde{\Omega}_{ij} = \Omega_{ij} - 2\varepsilon_{ijk}\omega_k; \quad \Omega_{ij} = \overline{\Omega_{ij}} - \varepsilon_{ijk}\omega_k; \quad A_s = \sqrt{6}\cos\Phi \qquad (12)$$

where:

$$\phi = \frac{1}{3}arc\,cos(\sqrt{6}W); \quad W = \frac{S_{ij}S_{jk}S_{ki}}{S^3}; \quad \tilde{S} = \sqrt{S_{ij}S_{ij}}$$
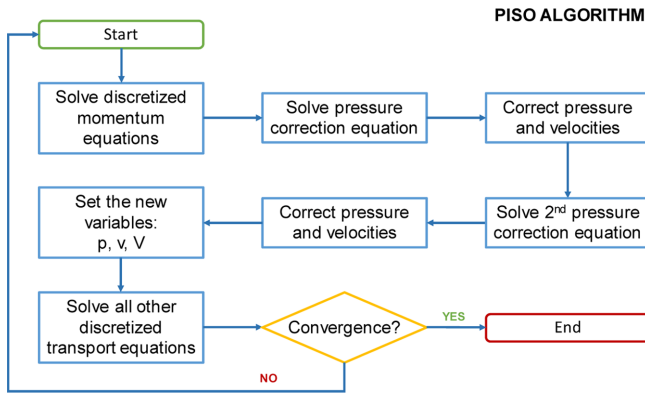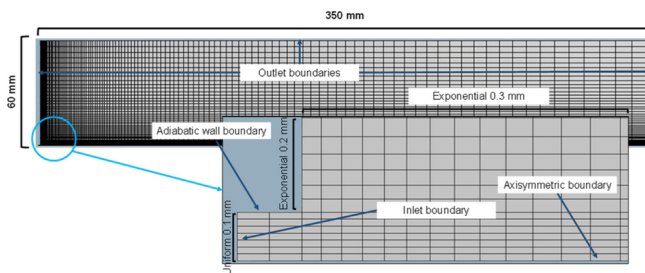
Fig. 3 PISO algorithm

Fig. 4 Mesh sketch for 1.5 mm of diameter outlet

Fig. 5 Nozzle diameters simulations by CFD

Finally, the resolution algorithm chosen to carry out iterations was PISO algorithm (pressure implicit with splitting of operators). This resolution algorithm is a pressure-velocity procedure developed for non-iterative computation of unsteady compressible flows. However, it was also adapted for the iterative solution of both, unsteady compressible and steady incompressible flow problems. It implies a step indicator/predictor, as simple algorithm method, and two corrective steps to get a fast convergence. In Fig. 3 is exposed a diagram with the steps followed by this resolution algorithm.

3. Optimum Diameter for CO_2 Outlets

Once the mathematical basis was stablished, different diameter sizes were simulated to get the optimum CO_2 outlet. It should be taken into account that larger outlets imply an increase of CO_2 consumption. This issue is of great importance with the aim of reducing not only environmental impact but also being more efficient economically. Hence, CO_2 outlets must to be smaller as possible.

The diameters tested were 0.5 mm, 1 mm and 1.5 mm, respectively. Afterwards, these tests were applied in a test bench with the aim of validating the mathematical models applied in the CFD software. In this way, they can be extrapolated to be used in the nozzle adapters developments to achieve the correct design. Besides basing on simulation and test bench results, the minimum CO_2 velocity to assist machining processes was established.

3.1 CFD Mesh and Boundaries

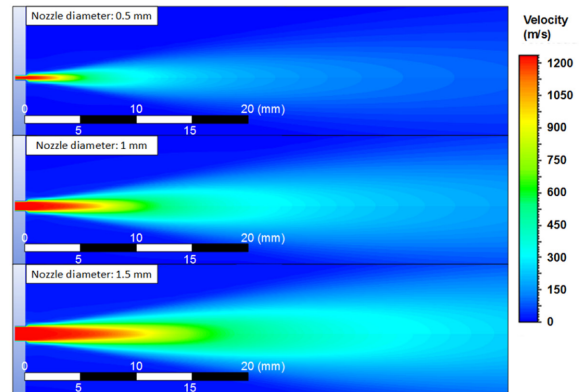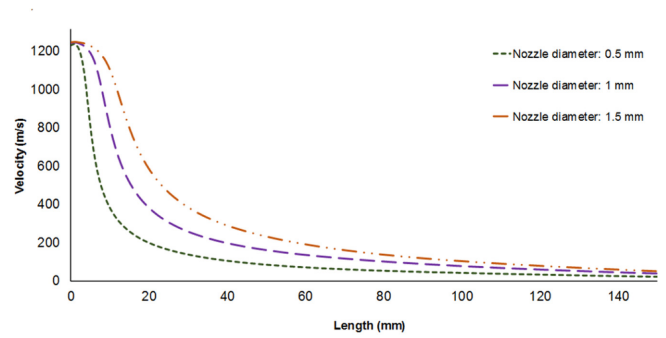Regarding CO_2 outlet simulations, different 2D quadratic axisymmetric meshes were made for each CO_2 outlet diameter. The total length of the meshes were 350 mm with an exponential nodes spacing of 0.2 mm for vertical axis and 0.3 mm for horizontal one. However, in the outlet nozzle zones, vertical nodes spacing was uniform with 0.1 mm. Regarding boundary conditions, it should be noted: constant pressure of 14 bars and turbulent intensity of 10% were supposed in the CO_2 inlet; CO_2 outlet walls were supposed as adiabatic walls; and remaining mesh boundaries was stablished as outlets with atmospheric pressure, backflow turbulent intensity of 2% and backflow turbulent length scale based on Eq. (13), where L is hydraulic diameter. In Fig. 4, an example with mesh characteristics and boundaries used for 1.5 mm outlet is summarized.

$$l = 0.07L \qquad (13)$$

3.2 Results and Discussion

Normal average velocities for the three outlet diameters were calculated in the CO_2 outlet symmetry axis. Fig. 5 shows a graphic with these velocities and their respective simulations. Average velocity at the first 20 mm was decreased until 6 times with a diameter of 0.5 mm and 3 times with one of 1 mm. However, with a diameter of 1.5 mm, only it was reduced by a half, that is, the velocity was maintained at 600 m/s in this point. It also should be noted that CO_2 tends to be spread in the atmosphere. In this line, the CO_2 injected with a diameter of 1.5 mm raised 30 mm of distance from the CO_2 inlet with 400 m/s.

3.3 Experimental Validation

Once velocity simulations were obtained, CO_2 outlet diameters were applied in a test bench to be compared with these simulations. This test bench, showed in Fig. 6, was composed by a board divided by quadratic sectors of 20×20 mm to be able measure distances; a high speed digital camera Olympus i-speed LT; a nozzle with the appropriate
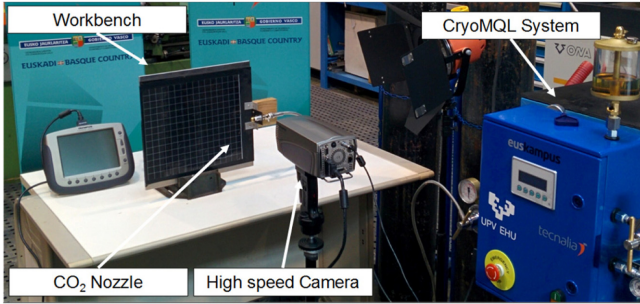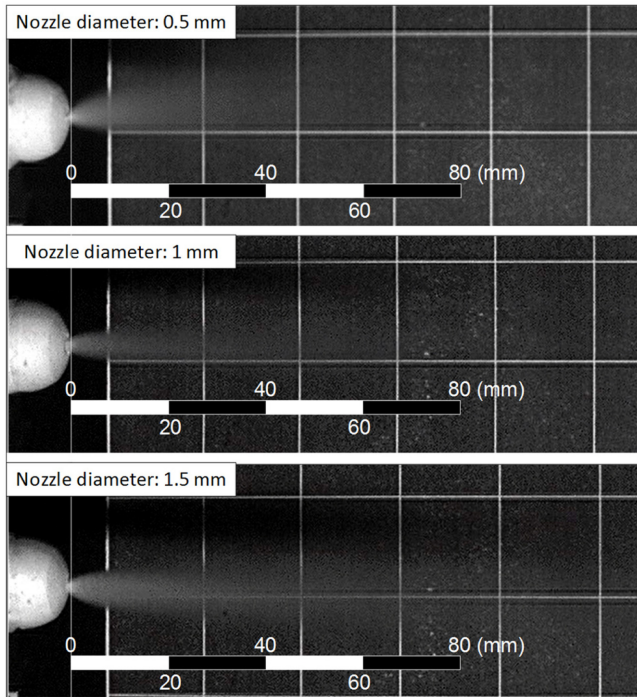
Fig. 6 Test bench used during the diameter tests

Fig. 7 Results obtained in the test bench

Fig. 8 Comparison CFD simulation with real images
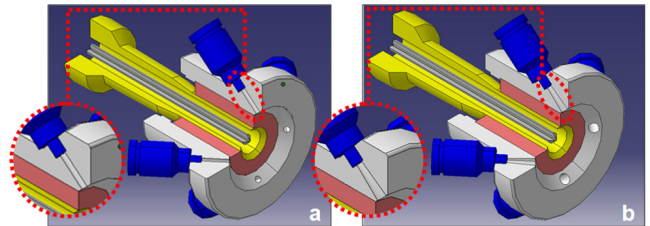
Fig. 9 Nozzle adaptor designs: (a) Convergent outlets adaptor, (b) Convergent-Divergent adaptor

diameter; a CO_2 injection system; and five tungsten spotlight with 1000 W of power each one. Acquisition parameters were stablished in 1,500 frames per second.

3.3.1 Results and Discussion

Results obtained for each CO_2 outlet diameter are shown in Fig. 7. In these tests, mainly it was appreciated CO_2 spread in the air. Spray distance with an outlet diameter of 0.5 mm reached 10 mm and with 1 mm outlet was risen 18 mm. However, with an outlet of 1.5 mm it was reached 40 mm of distance from the nozzle tip.

In order to validate the mathematical models chosen, real and simulation results were compared in Fig. 8. Both results showed a similar CO_2 spread, what indicates the validity of mathematical models used in the CFD software. Besides, taking into account the results obtained by Park et al. 2010[30] in which the maximum area fraction covered by MQL oil droplets happens at 30 mm from the nozzle tip, the optimal CO_2 length was determined. This distance only is overtaken by the nozzle provided with a diameter of 1.5 mm without spread, reaching 40 mm. Therefore, with the aim of obtaining
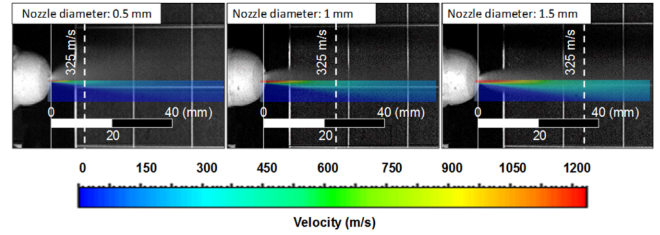
a balance between the maximum length got by CO_2 spray and the oil droplets concentration the optimal length was stablished at 35 mm. Moreover, applying this value to the comparison, the useful CO_2 velocity value to assist the oil micro-droplets spray or be injected in the cutting zone was determined. Based on this distance, the velocity was stablished in 325 m/s. Thus, in order to achieve CryoMQL technology, 1.5 mm diameter is the suitable size to be used in the nozzle adaptors.

4. CryoMQL Nozzle Development

Based on both CO_2 diameter outlet chosen and mathematical models validated to be used in this case, two nozzle adaptors were designed and simulated. Although they were designed following the same essence, they differ in CO_2 injection way. Both nozzle adapters have a central connection to be fixed on standard MQL nozzles; and also have four external fits where CO_2 channels are connected. However, CO_2 outlets are different, as it is shown in Fig. 9. The first adapter has CO_2 convergent outlets, whereas the second one has a convergent-divergent outlet (Laval nozzle). These options were chosen because on one hand according to classical fluid dynamics a smaller section implies higher fluid velocity but on the other, taking into account compressible fluid dynamics is possible higher velocities.

4.1 CFD Mesh and Boundaries

Regarding the CFD simulation, also an axisymmetric mesh was used as it is shown in Fig. 10. However, instead of using a uniform increase nodes spacing, the mesh model was divided in 5 blocks with different sizes and spacing. In Table 1 is detailed the meshing characteristics of each block. In both nozzle adapter simulations were used the same boundary conditions based on the previous simulations, that is: constant pressure of 14 bars for CO_2 inlets; all nozzle adapter walls were supposed as adiabatic walls; and outlets
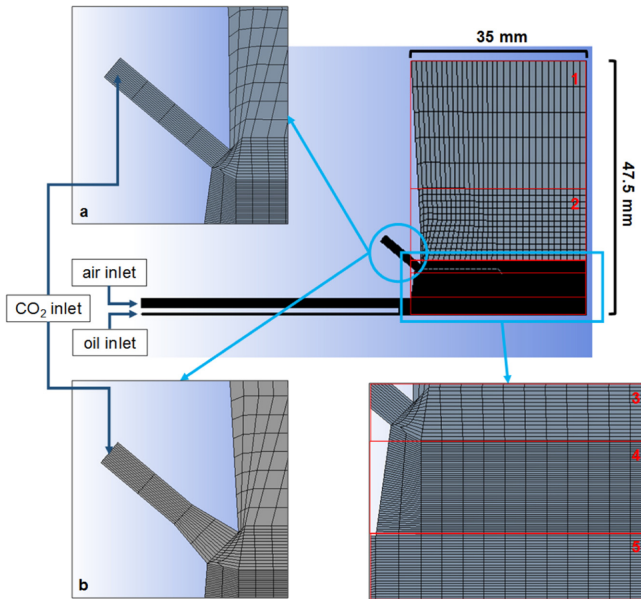
Fig. 10 Nozzle adaptor mesh: (a) Convergent outlet, (b) Convergent-Divergent outlet

Table 1 Blocks characteristics

Zones	Horizontal		Vertical	
	Length (mm)	Spacing (number)	Length (mm)	Spacing (number)
1	35	33	23.68	6
2	31.13	33	13.32	14
3	30	30	2.5	15
4	30.36	30	4.5	50
5	30.36	30	3	25

were stablished with atmospheric pressure, backflow turbulent intensity of 2%, and turbulent length scale based on Eq. (13). Besides in this case were used 6 bars for air inlet, and constant velocity 1.418×10^{-6} m/s for oil inlet (flow rate: 100 mL/h) to introduce MQL spray in the simulation.

4.2 Results and Discussion

Fig. 11 shows the simulations and a graphic with the normal averages velocities obtained for each nozzle analyzed. The velocities obtained are associated to the CryoMQL spray, that is, the velocity values represented in the graphic are taken in the symmetric axis from the nozzle tip. The minimum velocity to assist both the micro-oil droplets and the cutting process was stablished in the previous simulations (325 m/s). This value was reached at 9 mm for convergent-divergent nozzle and 14 mm for the other. From these points, the velocities increased until reach 475 m/s at 22 mm for convergent-divergent nozzle and 400 m/s at 23 mm for convergent one. However, it should be noted that although with convergent-divergent nozzle larger velocities were reached, also the spray spread was bigger. In particular, spray spot for convergent-divergent nozzle had ≈ 15.6 mm of diameter and ≈ 9 mm for convergent one. This supposes a spray concentration in the cutting zone of 1.7 times better for convergent nozzle in which its velocity is over 325 m/s. Thus, this design is the appropriate to be used during machining processes.
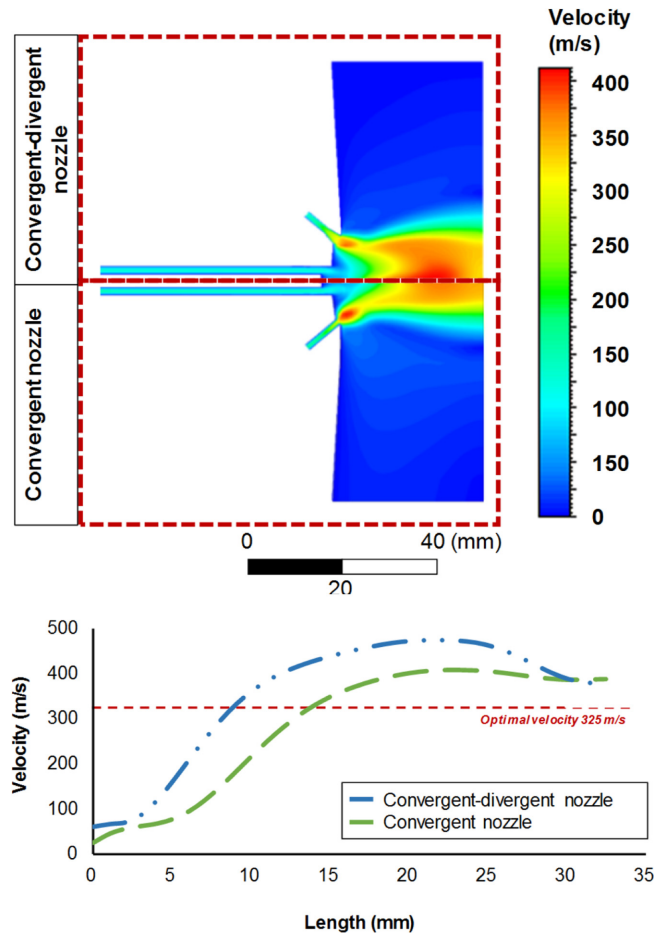

Fig. 11 Nozzle adaptor simulations made by CFD

5. Experimental Validation

Once the nozzle adaptor was designed and manufactured, it is needed to take an industrial vision of the development and test its behavior in real machining operations. In this line, experimental tests were carried out using Inconel 718 aged (45 HRc). This nickel alloy is a representative turbomachinery alloy which supposes a significant portion of the manufacturing costs of aircraft engine components. It is characterized by high strength and high wear and corrosion resistance at high temperatures.[31] On the other hand, this alloy is considered as hard-to-cut material due to its low thermal conductivity and its austenitic matrix is hardened after each tool pass. This behavior causes premature tool wear and poor material removal rates. Notch and crater wear is common problem during cutting these materials.[32-34] Hence, the use of cutting fluids become relevant.

5.1 Experimental Setup and Test Performance

Tests were performed in a Kondia HS1000 three axis-machining center in which CryoMQL lubricooling technology applied with the nozzle developed was compared with dry machining, MQL lubrication, CO_2 cooling and wet machining. The oil flow rate used during MQL and CryoMQL machining was 100 mL/h. Liquid CO_2 was injected with 14 bars. In Fig. 12 experimental setup is shown.

Tool used was a bull nose finishing end mill with 16 mm of diameter and two cutting edges. Carbide inserts coated with TiN were
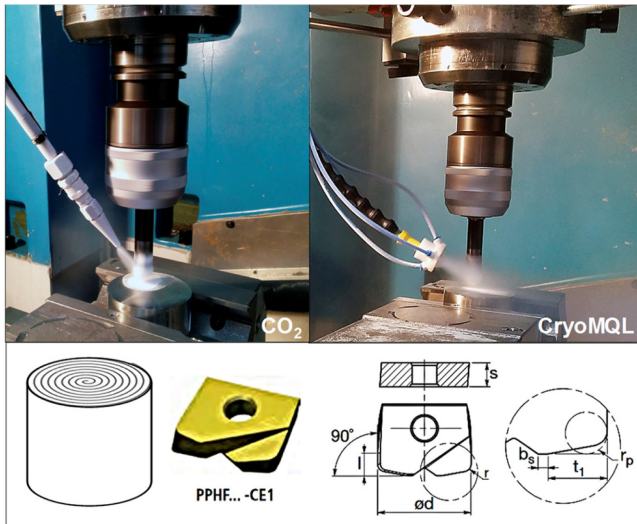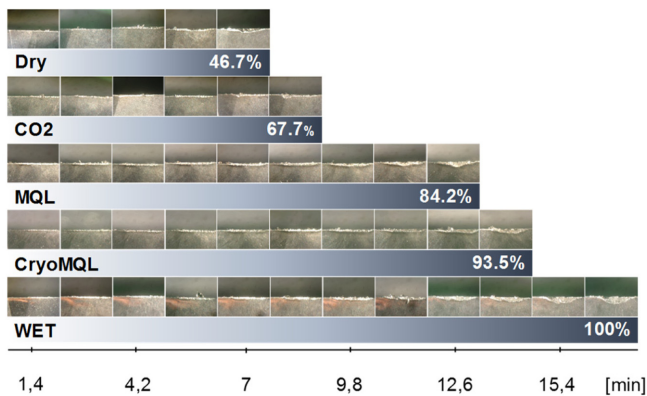
Fig. 12 Experimental setup

Fig. 13 Results obtained

used. In order to amplifying the different lubricooling effects aggressive cutting conditions were chosen. In particular, cutting speed (V_c) of 120 m/min, feed rate (f) of 0.12 mm/teeth, radial depth (a_e) of 3 mm and depth of cut (a_p) of 0.2 mm were used. As wear criterion, the tests were stopped at a flank wear of $V_B = 0.2$ mm, because higher values demonstrated the surface integrity can be affected in this type of alloys.[31] Spiral face milling was chosen as machining strategy. After each spiral path, flank wear (V_{Bmax}) was measured with a Nikon SMZ-2T microscope.

5.2 Results and Discussion

Results obtained are shown in Fig. 13. Using CO_2 tool life increases in comparison with dry machining due to cutting temperature decrease. However, this thermal charge decrease is not enough to achieve a feasible process. In fact, taking as reference wet machining, tool life represents only a 67.7%. On the other hand, when MQL is applied, this value increases until 84.2% what indicates that mechanical charges which involves tool wear are greater than thermal ones.

However, lubrication effects and thermal effects should be combined to achieve a feasible solution. Results show that combining CO_2 and MQL with the nozzle adaptor developed (CryoMQL) tool life increases till 93.5%. This supposes the possibility of machining during 15 minutes, that is, with CryoMQL technique the tool reaches the normalized tool life duration.

Besides in comparison with the other alternatives, during the tool wear evolution shows a regular increase without unexpected catastrophic fail what makes stable the cutting process. Thus, CryoMQL is presented as a feasible solution to avoid the use of oil mineral emulsions as cutting fluids. In this way, a balance between technical and environmental matters is achieved.

6. Conclusions

In this paper, numerical and experimental analyses were made for achieving environmental and efficient lubricooling technique based on MQL and CO_2 combination (CryoMQL). For this, firstly several CO_2 diameter outlets were simulated by CFD and validated experimentally to obtain the optimal CO_2 velocity in order to assist machining processes. Afterwards based on these results and mathematical basis, authors proposed and analyzed numerically two nozzle adaptors. Finally, Inconel 718 was milled to validate the chosen nozzle adaptor. For this, several lubricooling techniques were compared. The main conclusions obtained from the numerical and experimental studies are listed below:

· The minimum velocity in which CO_2 is useful to assist micro oil droplets and being used in cutting processes was obtained based on the comparison between numerical and experimental tests made. This value was stablished in 325 m/s. According to the diameter outlet chosen, this value was reached in different distances, being the suitable size 1.5 mm. With this size, CO_2 reaches 35 mm of distance without being spread in the atmosphere.

· Although convergent-divergent adaptor nozzle reaches higher cutting fluid velocities than convergent one, also it is important to focalize the spray spot. In this line, convergent nozzle has 1.7 times more focalized spray spot in which cutting fluid velocity is over 325 m/s.

· According to experimental tests made by milling Inconel 718, wet machining is the best option from a technical point of view. However, environmental issues have to be taken into account. In this line, CryoMQL technology presents a balance between technical and environmental issues reaching 15 min of tool life.

ACKNOWLEDGEMENT

REFERENCES

1. Klocke, F., Krämer, K., Sangermann, H., and Lung, D., "Thermo-Mechanical Tool Load during High Performance Cutting of Hard-to-Cut Materials," Procedia CIRP, Vol. 1, pp. 295-300, 2012.

2. Bhatt, A., Attia, H., Vargas, R., and Thomson, V., "Wear Mechanisms of WC Coated and Uncoated Tools in Finish Turning of Inconel 718," Tribology International, Vol. 43, No. 5, pp. 1113-1121, 2010.

3. Hosokawa, A., Ueda, T., Onishi, R., Tanaka, R., and Furumoto, T., "Turning of Difficult-to-Machine Materials with Actively Driven Rotary Tool," CIRP Annals-Manufacturing Technology, Vol. 59, No. 1, pp. 89-92, 2010.

4. Thakur, D. G., Ramamoorthy, B., and Vijayaraghavan, L., "Study on the Machinability Characteristics of Superalloy Inconel 718 during High Speed Turning," Materials and Design, Vol. 30, No. 5, pp. 1718-1725, 2009.

5. Costes, J. P., Guillet, Y., Poulachon, G., and Dessoly, M., "Tool-Life and Wear Mechanisms of CBN Tools in Machining of Inconel 718," International Journal of Machine Tools and Manufacture, Vol. 47, pp. 1081-1087, 2007.

6. Klocke, F., Klink, A., Veselovac, D., Keith, D., Leung, S., et al., "Turbomachinery Component Manufacture by Application of Electrochemical, Electro-Physical and Photonic Processes," CIRP Annals-Manufacturing Technology, Vol. 63, pp. 703-706, 2014.

7. Klocke, F. and Eisenblatter, G., "Dry Cutting," CIRP Annals-Manufacturing Technology, Vol. 46, No. 2, pp. 519-526, 1997.

8. Jerold, B. D. and Kumar, M. P., "Experimental Investigation of Turning AISI 1045 Steel Using Cryogenic Carbon Dioxide as the Cutting Fluid," Journal of Manufacturing Processes, Vol. 13, No. 2, pp. 113-119, 2011.

9. Byrne, G., Dornfeld, D., and Denkena, B., "Advancing Cutting Technology," CIRP Annals-Manufacturing Technology, Vol. 52, No. 2, pp. 483-507, 2003.

10. Cetin, M., Ozcelik, B., Kuram, E., and Demirbas, E., "Evaluation of Vegetable Based Cutting Fluids with Extreme Pressure and Cutting Parameters in Turning of AISI 304L by Taguchi Method," Journal of Cleaner Production, Vol. 19, No. 17, pp. 2049-2056, 2011.

11. Park, K., Olortegui-Yume, J., Yoon, M., and Kwon, P., "A Study on Droplets and Their Distribution for Minimum Quantity Lubrication (MQL)," International Journal of Machine Tools and Manufacture, Vol. 50, No. 9, pp. 824-833, 2010.

12. Shokrani, A., Dhokia, V., and Newman, S., "Environmentally Conscious Machining of Difficult-to-Machine Materials with Regard to Cutting Fluids," International Journal of Machine Tools and Manufacture, Vol. 57, pp. 83-101, 2012.

13. Herrmann, C., Schmidt, C., Kurle, D., Blume, S., and Thiede, S., "Sustainability in Manufacturing and Factories of the Future," Int. J. Precis. Eng. Manuf.-Green Tech., Vol. 1, No. 4, pp. 283-292, 2014.

14. Jang, D., Jung, J., and Seok, J., "Modeling and Parameter Optimization for Cutting Energy Reduction in MQL Milling Process," Int. J. Precis. Eng. Manuf.-Green Tech., Vol. 3, No. 1, pp. 5-12, 2016.

15. Dureja, J., Singh, R., Singh, T., Dogra, M., and Batti, M., "Performance Evaluation of Coated Carbide Tool in Machining of Stainless Steel (Aisi 202) under Minimum Quantity Lubrication (MQL)," Int. J. Precis. Eng. Manuf.-Green Tech., Vol. 2, No. 2, pp. 123-129, 2015.

16. De Lacalle, L. L., Angulo, C., Lamikiz, A., and Sanchez, J., "Experimental and Numerical Investigation of the Effect of Spray Cutting Fluids in High Speed Milling," Journal of Materials Processing Technology, Vol. 172, No. 1, pp. 11-15, 2006.

17. Pereira, O., Rodríguez, A., Fernández-Abia, A., Barreiro, J., and De Lacalle, L. L., "Cryogenic and Minimum Quantity Lubrication for an Eco-Efficiency Turning of AISI 304," Journal of Cleaner Production, Vol. 139, pp. 440-449, 2016.

18. Pusavec, F., Deshpande, A., Yang, S., M'Saoubi, R., Kopac, J., et al., "Sustainable Machining of High Temperature Nickel Alloy-Inconel 718: Part 1-Predictive Performance Models," Journal of Cleaner Production, Vol. 81, pp. 255-269, 2014.

19. Machai, C., Iqbal, A., Biermann, D., Upmeier, T., and Schumann, S., "On the Effects of Cutting Speed and Cooling Methodologies in Grooving Operation of Various Tempers of I2-Titanium Alloy," Journal of Materials Processing Technology, Vol. 213, No. 7, pp. 1027-1037, 2013.

20. Stephenson, D., Skerlos, S., King, A., and Superkar, S., "Rough Turning Inconel 750 with Supercritical CO_2-based Minimum Quantity Lubrication," Journal of Materials Processing Technology, Vol. 214, pp. 673-680, 2014.

21. Supekar, S., Clarens, A., Stephenson, D., and Skerlos, S., "Performance of Supercritical Carbon Dioxide Sprays as Coolants and Lubricants in Representative Metalworking Operations," Journal of Materials Processing Technology, Vol. 212, No. 12, pp. 2652-2658, 2012.

22. Clarens, A., Hayes, K., and Skerlos, S., "Feasibility of Metalworking Fluid Delivered in Supercritical Carbón Dioxide," Journal of Manufacturing Processes, Vol. 8, No. 1, pp. 47-53, 2006.

23. Jackson, D. P., "Nozzle Device and Method for Forming Cryogenic Composite Fluid Spray," US Patent, No. 7389941 B2, 2008.

24. Shih, T. H., Liou, W. W., Shabbir, A., Yang, Z., and Zhu, J., "A New K-E Eddy Viscosity Model for High Reynolds Number Turbulent Flows," Computers and Fluids, Vol. 24, No. 3, pp. 227-238, 1995.

25. Cotas, C., Silva, R., García, F., Faia, P., Asendrych, D., et al., "Application of Different Low-Reynolds K-ε Turbulence Models to Model the Flow of Concentrated Pulp Suspension in Pipes," Procedia Engineering, Vol. 102, pp. 1326-1335, 2015.

26. Duchosal, A., Serra, T., Leroy, R., and Louste, C., "Numerical Steady Prediction of Spitting Effect for Different Internal Canalization Geometries Used in MQL Machining Strategy," Journal of Manufacturing Processes, Vol. 20, pp. 149-161, 2015.

27. Obikawa, T., Asano, Y., and Kamata, Y., "Computer Fluid Dynamics Analysis for Efficient Spraying of Oil Mist in Finishing-

Turning of Inconel 718," International Journal of Machine Tools and Manufacture, Vol. 49, No. 12, pp. 971-978, 2009.

28. Reynolds, W., "Fundamentals of Turbulence for Turbulence Modeling and Simulation," http://oai.dtic.mil/oai/oai?verb=getRecord &metadataPrefix=html&identifier=ADP005793 (Accessed 24 December 2016)

29. Shih, T. H., Zhu, J., and Lumley, J. L., "A New Reynolds Stress Algebraic Equation Model," Computer Methods in Applied Mechanics and Engineering, Vol. 125, No. 1, pp. 287-302, 1995.

30. Park, K. H., Olortegui-Yume, J., Yoon, M. C., and Kwon, P., "A Study on Droplets and Their Distribution for Minimum Quantity Lubrication (MQL)," International Journal of Machine Tools and Manufacture, Vol. 50, No. 9, pp. 824-833, 2010.

31. De Lacalle, L. L., Perez-Bilbatua, J., Sánchez, J., Llorente, J., Gutierrez, A., et al., "Using High Pressure Coolant in the Drilling and Turning of Low Machinability Alloys," Journal of Advanced Manufacturing Technology, Vol. 16, No. 2, pp. 85-91, 2000.

32. Fernández-Valdivielso, A., De Lacalle, L. L., Urbikain, G., and Rodríguez, A., "Detecting the Key Geometrical Features and Grades of Carbide Inserts for the Turning of Nickel-Based Alloys Concerning Surface Integrity," Journal of Mechanical Engineering Science, Article ID: 0954406215616145, 2015.

33. Urbicain, G., Palacios, J., Fernández, A., Rodríguez, A., De Lacalle, L. L., et al., "Stability Prediction Maps in Turning of Difficult-to-Cut Materials," Procedia Engineering, Vol. 63, pp. 514-522, 2013.

34. Choudhury, I. and El-Baradie, M., "Machinability of Nickel-Base Super Alloys: A General Review," Journal of Materials Processing Technology, Vol. 77, No. 1, pp. 278-284, 1998.